International Journal of Minerals, Metallurgy and Materials
Volume 27, Number 12, December 2020, Page 1695
https://doi.org/10.1007/s12613-020-2169-y

Electrochemical preparation of the Fe–Ni36 Invar alloy from a mixed oxides precursor in molten carbonates

Yan-peng Dou, Di-yong Tang, Hua-yi Yin, and Di-hua Wang

School of Resource and Environmental Sciences, Wuhan University, Wuhan 430072, China
(Received: 31 May 2020; revised: 14 August 2020; accepted: 17 August 2020)

Abstract: The Fe–Ni36 alloy was prepared via the one-step electrolysis of a mixed oxides precursor in a molten Na_2CO_3–K_2CO_3 eutectic melt at 750°C, where porous Fe_2O_3–NiO pellets served as the cathode and the Ni10Cu11Fe alloy was an inert anode. During the electrolysis, NiO was preferentially electro-reduced to Ni, then Fe_2O_3 was reduced and simultaneously alloyed with nickel to form the Fe–Ni36 alloy. Different cell voltages were applied to optimize the electrolytic conditions, and a relatively low energy consumption of 2.48 $kW{\cdot}h{\cdot}kg^{-1}$ for production of FeNi36 alloy was achieved under 1.9 V with a high current efficiency of 94.6%. The particle size of the alloy was found to be much smaller than that of the individual metal. This process provides a low-carbon technology for preparing the Fe–Ni36 alloy via molten carbonates electrolysis.

Keywords: molten carbonates; cyclic voltammetry; electro-reduction; inert anode; Invar36 alloy

1. Introduction

Iron and Ni alloys possessing excellent mechanical properties and low cost are one of the most widely used structure materials. For example, near room temperature, Fe–Ni alloys with 30wt%–40wt% Ni have coefficients of thermal expansion (CTEs) lower than those of pure Fe (CTE = 12×10^{-6} $°C^{-1}$) and Ni (CTE = 13×10^{-6} $°C^{-1}$). In particular, the Fe–Ni alloys with 36wt% Ni exhibit the lowest CTE (approximately 1×10^{-6} $°C^{-1}$) among all Fe–Ni alloys [1–3]. The Fe–Ni36 alloy and those of similar composition are denoted "Invar alloys." The Invar alloys are widely used in various applications, such as optical and laser measuring systems, bimetallic strips, shadow masks, precision instruments, large molds for aerospace, and storage vessels for liquefied natural gas [1,3], because of their high temperature strength and oxidation and corrosion resistance. Currently, the preparation of Ni–Fe alloys involves multiple steps, including a carbothermic reduction route for preparing Fe and Ni and an alloying process in which Ni and Fe are mixed at a high temperature [4].

Eletro-deoxidation of solid oxides in molten salts, also called the FFC Cambridge Process, is a straightforward way to prepare metals and/or alloys [5–7]. A variety of alloys have been successfully prepared from their corresponding oxides or oxide mixtures, i.e., TiFeNi [8], TiNi [9–10], $TbFe_2$ [11], $LaNi_5$ [12], $TbNi_5$ [13], and NiAl [14]. Inspired by the FFC Cambridge process, researchers substituted molten hydroxides [15] and carbonates [16] for molten halide to prepare other noble metals, such as Fe, Co, and Ni [16–18]. The merit of replacing molten halide (e.g., $CaCl_2$) is the opportunity to use a cost-effective inert anode. The drawback of using molten hydroxide and carbonate is the relatively narrow electrochemical window limiting the preparation of reactive metals [19–20].

A homemade Ni10Cu11Fe inter-anode can serve as a long-lasting oxygen-evolution anode to electrochemically split Fe_2O_3, NiO, and Co_3O_4 into Fe, Ni, Co, and oxygen [16–18]. Thermodynamically, Ni and other metals having similar electronegativity can be reduced to their corresponding metals/alloys in molten Na_2CO_3–K_2CO_3. To test the durability of the long-lasting inert anode, the oxidation behavior of the Ni10Cu11Fe inter-anode was investigated, revealing that a three-layer structure oxide scale plays a central role in maintaining the functionality of the inert anode [21–22]. To date, no paper has reported the preparation of ferro-alloys in molten carbonate, and the possibility of the alloying process still needs to be confirmed. Since the wide application of Fe-based alloys, a molten carbonate with a low-cost inert anode could pave an environmentally friendly way to preparing

Corresponding author: Di-hua Wang E-mail: wangdh@whu.edu.cn

value-added alloys in one step.

Herein, we report the preparation of the Fe–Ni36 alloy via one-step electrolysis of a mixed oxides precursor in molten carbonates. The reduction process of the Fe_2O_3–NiO mixture in molten Na_2CO_3–K_2CO_3 and the optimized electrolytic condition, current efficiency, and energy consumption were studied using cyclic voltammetry and constant cell voltage electrolysis.

2. Experimental

2.1. Materials and chemicals

Fe_2O_3 and NiO powders (Fe : Ni mass ratio of 64:36; analytical purity; Sinopharm Chemical Regent Co. Ltd., China) were ball-mixed for 12 h, and the mixed oxides were mixed with 20wt% NH_4HCO_3 manually and made into pellets by die-pressing at a pressure of 6 MPa. Afterward, the oxide pellets were sintered in a muffle furnace at 800°C for 2 h to ensure a reasonable mechanical strength. The NH_4HCO_3 was added to increase the porosity of the pellets through the decomposition of NH_4HCO_3 at a high temperature. Then, the sintered pellets were attached to an iron wire (2 mm in diameter) working as a cathode. A Ni10Cu11Fe alloy rod (20 mm in diameter) was applied as an anode, and the detailed preparation process was reported in our previous work [18]. A 500 g eutectic Na_2CO_3–K_2CO_3 mixture (59:41 in molar ratio; analytical purity; Sinopharm Chemical Regent Co. Ltd., China) was placed in an alumina crucible in a closed-end, sealed steel reactor. Before the electrolysis, the mixed salts were heated to 850°C to melt the electrolyte, and then the temperature was lowered to 750°C for electrochemical measurements. Pre-electrolysis was conducted under a constant cell voltage of 1.8 V with a Ni10Cu11Fe inert anode and a nickel sheet cathode for 2 h to remove the residual water and, if any, other impurities from the salts. All experiments were performed under an argon flow (>99.999%; Wuhan Iron and Steel Group Corp., China).

2.2. Cyclic voltammetry

A three-electrode setup was applied to conduct cyclic voltammetry (CV) measurements controlled by a CHI1140a electrochemical workstation (Shanghai Chenhua Instrument Co. Ltd., China) to investigate the reduction mechanisms of NiO and Fe_2O_3. A nickel wire (1 mm in diameter, 5–6 mm in length, immersed in the melt) and an oxide coated nickel or iron wire were used as the working electrodes. The reference electrode was a silver wire dipped in a Ag_2SO_4 (2mol%) eutectic melt (Li_2CO_3 : Na_2CO_3 : K_2CO_3 molar ratio = 43.5:25:31.5) in a one-end closed mullite tube, and a Ni10Cu11Fe alloy rod was used as the counter electrode. The oxide coated nickel or iron wire was fabricated by repeatedly dipping a nickel wire (1 mm in diameter) into an oxide- or mixed-oxide-ethanol suspension (3 g of oxides in 5 mL of ethanol under sonication), then the ethanol was dried, giving an oxide powder coated metal wire working electrode. Unless otherwise specified, all potentials were collected with respect to the reference electrode.

2.3. Two-electrode constant cell voltage electrolysis

Two-electrode constant cell voltage electrolysis was conducted to prepare the Fe–Ni36 alloy from the pre-sintered Fe_2O_3–NiO mixture pellets. The sintered Fe_2O_3–NiO pellets (~0.6 g) were wrapped with a nickel foam and then attached to an iron wire (2 mm in diameter) working as the cathode in conjunction with a Ni10Cu11Fe inert anode. Constant electrolysis was applied between the cathode and anode in a potential range from 1.0 to 2.2 V, and the electrolysis was controlled using a DC power system (Shenzhen Neware Electronic Ltd., China). After electrolysis, the obtained products were washed in distilled water to remove the residual molten salt, followed by vacuum-drying and conservation in ethanol. The electrolytic samples were characterized using scanning electron microscopy (SEM, FEI Sirion field emission), X-ray diffraction spectroscopy (XRD, Shimadzu X-ray 6000 with Cu $K_{\alpha 1}$ radiation at λ = 0.15405 nm), and energy-dispersive X-ray spectroscopy (EDX, EDAX GENESIS 7000).

3. Results and discussion

3.1. CV measurements

Cyclic voltammetry was conducted to investigate the reduction mechanisms of NiO and Fe_2O_3 in the Na_2CO_3–K_2CO_3 eutectic melt. As shown in Fig. 1, only one reduction peak was present for the NiO coated nickel working electrode, indicating a one-step reduction process for NiO. For the Fe_2O_3 coated iron working electrode, two reduction peaks were observed for Fe_2O_3 reduction, which are related to electrochemical intercalation of Na^+ into Fe_2O_3 to form $NaFe_2O_3$ and $NaFeO_2$ (reactions (1) and (2)) and electro-reduction of $NaFeO_2$ to iron metal (reaction (3)) [23]. The reduction peak of NiO began at −1.34 V (peak a3 in Fig. 1, reaction (4)), which was close to the first reduction peak of Fe_2O_3 (peak a1 in Fig. 1, −1.40 V), suggesting that NiO can be more easily electro-reduced to metal than Fe_2O_3.

$$Fe_2O_3 + Na^+ + e = NaFe_2O_3 \quad (1)$$

$$2NaFe_2O_3 + Na^+ + e = 3NaFeO_2 + Fe \quad (2)$$

$$NaFeO_2 + 3e = Fe + Na^+ + 2O^{2-} \quad (3)$$

$$NiO + 2e = Ni + O^{2-} \quad (4)$$

3.2. Two-electrode constant cell voltage electrolysis

As shown in Fig. 2, NiO reacted with Fe_2O_3 to form $NiFe_2O_4$ at a high temperature of 800°C, and the excess amount of Fe_2O_3 still maintained the original form.

Constant cell voltage electrolysis was used to reduce the

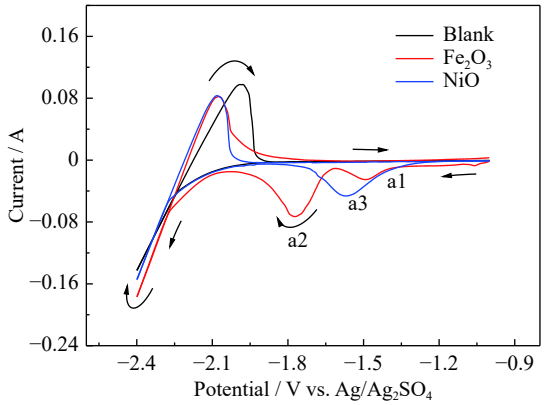

Fig. 1. Cyclic voltammograms of oxides coated electrodes at 750°C with a scan rate of 100 mV/s.

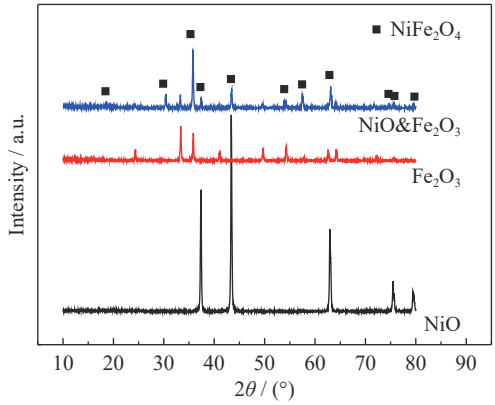

Fig. 2. XRD patterns of Fe_2O_3, NiO, and the mixed oxides of Fe_2O_3 and NiO ($NiO\&Fe_2O_3$) after sintering at 800°C for 2 h.

mixed oxide precursor. Fig. 3 shows the XRD patterns of the electrolytic products under cell voltages from 1.0 to 2.2 V for 11 h. Under 1.5 V, the major diffraction peaks of NiO, Fe_2O_3, and $NiFe_2O_4$ disappeared, suggesting that reduction occurred. The theoretical decomposition voltage for NiO at 750°C is 0.76 V, and it can be electro-reduced at a low cell voltage of 0.9 V [18]. The three new main diffraction peaks located at 44.5°, 51.8°, and 76.4° should ascribe to the freshly formed Ni, while other peaks located at 21.3° 29.6°, 33.5°, and 36.9° should be attributed to the intermediate compounds $NaFe_2O_3$ and $NaFeO_2$ [23]. When the cell voltage increased to 1.8 V, only the three main diffraction peaks were detected, indicating that the intermediate compounds were electro-reduced completely. Note that no Fe was observed under different cell voltages, suggesting that the reduction of iron compounds and generation of Ni–Fe_x alloys occurred simultaneously (Ni and the Fe–Ni36 alloy have identical characteristic diffraction peaks). This finding means that the reduction of Fe on the preformed Ni directly resulted in formation of Ni–Fe alloys. As the Ni–Fe solid solution formed, the main diffraction peaks negatively shifted to 43.9°, 51.2°, and 75.3°, respectively.

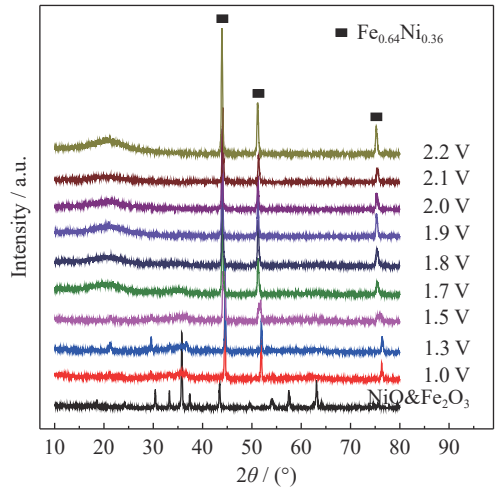

Fig. 3. XRD patterns of the electrolytic products obtained from the indicated constant cell voltages electrolysis experiments at 750°C in a Na_2CO_3–K_2CO_3 eutectic melt.

The SEM images of the electrolytic products obtained under different cell voltages are shown in Fig. 4. Under a cell voltage lower than 1.5 V (Figs. 4(a)–4(c)), the particles were uniform and the SEM images of the samples were similar. When the cell voltage was increased to 1.7–1.8 V (Figs. 4(d)–4(e)), coral-like metal structures began to appear [23]. As the cell voltage increased from 1.9 to 2.2 V (Figs. 4(f)–4(i)), a uniform coral-like structure was observed, suggesting that the mixed oxides had been completely reduced to alloys. Therefore, a cell voltage of 1.9 V was selected for investigating the reduction process of the mixed oxides in detail.

The XRD patterns of samples obtained under 1.9 V for different electrolysis durations are shown in Fig. 5. Before electrolysis, the pellet consisted of $NiFe_2O_4$ and Fe_2O_3. After 0.5 h, weak diffraction peaks of nickel metal were detected, and their intensity increased with increasing electrolysis time from 0.5 to 4 h. After 4 h, the diffraction peaks of $NiFe_2O_4$ disappeared, and the major diffractions peaks came from the Fe–Ni alloy. After electrolysis for 11 h, the oxides were fully reduced to form the Fe–Ni36 alloy. Notably, the main diffraction peaks also negatively shifted with a prolonged electrolysis time, which suggested that iron was progressively reduced and combined with Ni to form a Ni–Fe solid solution.

The SEM images of the mixed oxides precursor and the electrolytic products obtained under 1.9 V with different electrolysis times are shown in Fig. 6. Before electrolysis, the mixed oxides were irregular particles (Fig. 6(a)), and no obvious change was observed (Figs. 6(b) and 6(c)) after 1 h. After electrolyzed for 2 h (Fig. 6(d)), aggregation occurred between the particles. Larger granules were observed after 4 h (Fig. 6(e)), suggesting that nickel metal was obtained. After 6 h, a coral-like morphology was observed (Fig. 6(f)). The particles grew larger after 8 h (Fig. 6(g)), and the remaining fine particles became fewer. After 11 h (Figs. 6(h)

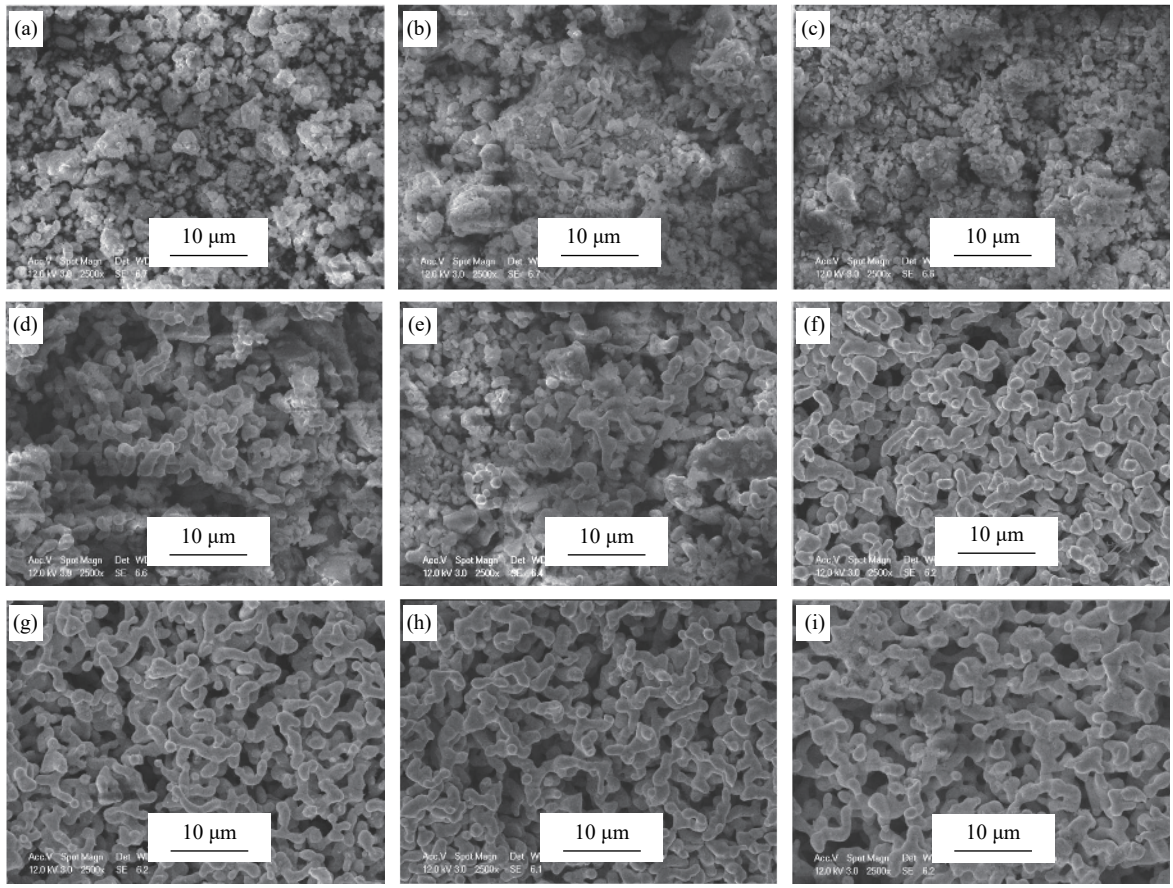

Fig. 4. SEM images of the obtained products of NiO–Fe_2O_3 mixed oxides pellets after electrolysis under constant cell voltages of (a) 1.0 V, (b) 1.3 V, (c) 1.5 V, (d) 1.7 V, (e) 1.8 V, (f) 1.9 V, (g) 2.0 V, (h) 2.1 V, and (i) 2.2 V at 750°C in a Na_2CO_3–K_2CO_3 eutectic melt for 11 h.

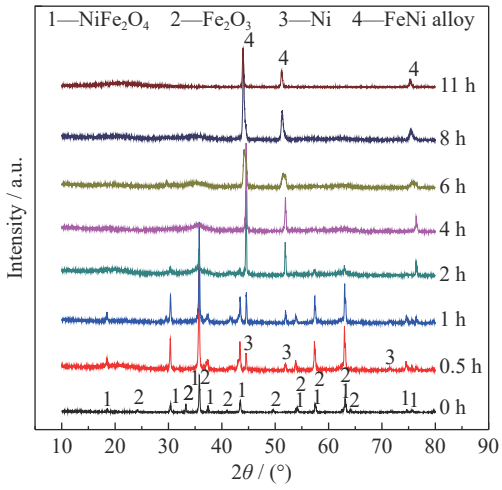

Fig. 5. XRD patterns of the obtained products of NiO and Fe_2O_3 mixed oxides pellets after electrolysis under a constant cell voltage of 1.9 V over the indicated electrolysis times at 750°C in a Na_2CO_3–K_2CO_3 eutectic melt.

and 6(i)), the particles continually grew and linked with each other, indicating that the mixed oxides were fully electro-reduced to Fe–Ni36.

Fig. 7 displays the SEM images of the electro-reduced nickel, iron, and Fe–Ni36 alloy obtained in molten carbonates (Na_2CO_3–K_2CO_3) at 750°C. The particle sizes of the electrolytic products were larger than those of their corresponding oxide precursors. For NiO, the morphology of the electrolytic nickel metal normally exhibited nodular particles with a particle size of 5–10 μm (Fig. 7(a)). The electrolytic Fe exhibited an interconnected coral-like morphology with a particle size range of 5–10 μm (Fig. 7(b)). For the mixed oxides of NiO–Fe_2O_3, the electrolytic alloy had a similar morphology with the coral-like sponge iron (Fig. 7(c)), but its particle size range was 1–2 μm, which was smaller than that of iron. According to the phase diagram of Fe–Ni, Ni and Fe form a solid solution at 750°C, revealing that the electrolytic product was the Fe–Ni36 alloy and not the separated Ni and Fe. Interestingly, the Ni–Fe alloy particles were obviously smaller than the individual metal particles at the same temperature, which should be closely related to the formation process of the Ni–Fe alloy. As discussed above, NiO is preferentially reduced to the Ni cation during the electrochemical reduction of the mixed oxides. Nearby iron oxides are reduced and the fresh Fe atoms diffuse to the Ni cation to form a Ni–Fe solution. The mobility of the Ni–Fe cation is pos-

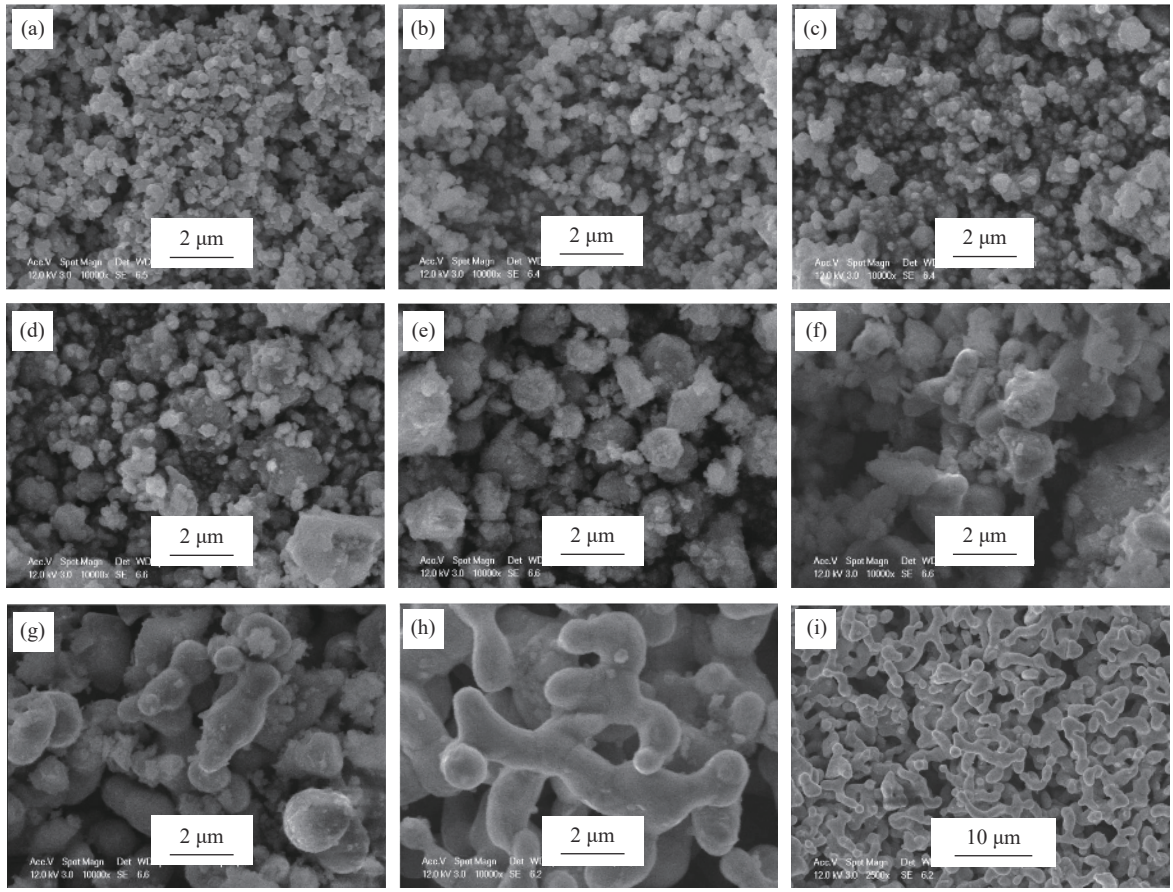

Fig. 6. SEM images of the obtained products of NiO and Fe_2O_3 mixed oxides after electrolysis under constant cell voltages of 1.9 V with different electrolysis times of (a) 0 h, (b) 0.5 h, (c) 1 h, (d) 2 h, (e) 4 h, (f) 6 h, (g) 8 h, and (h, i) 11 h at 750°C in a Na_2CO_3–K_2CO_3 eutectic melt.

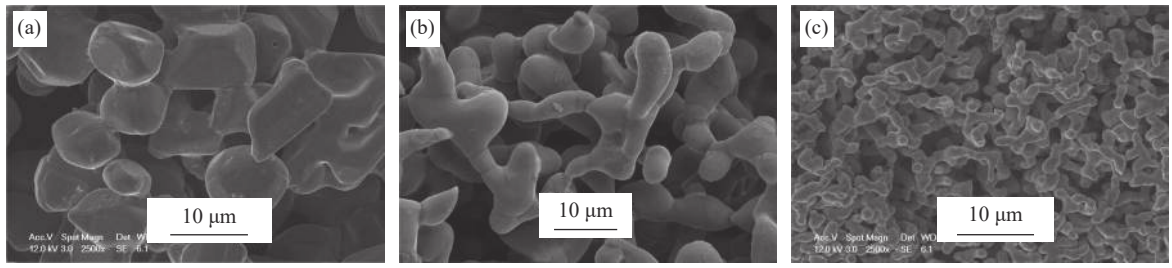

Fig. 7. SEM images of the electro-reduced (a) nickel, (b) iron, and (c) Fe–Ni36 alloy prepared at 750°C in a Na_2CO_3–K_2CO_3 eutectic melt.

sibly lower than that of the Ni or Fe cation. On the other hand, the reduction of the iron oxide intermediate compound is more sluggish, so it might become a diffusion barrier for the preferentially reduced Ni and Ni–Fe.

Fig. 8 shows the digital photos of NiO–Fe_2O_3 mixed oxide pellets before (left) and after (right) electrolyzed under 1.9 V for 11 h at 750°C in a Na_2CO_3–K_2CO_3 eutectic melt. The electrolytic product had metallic luster and good conductivity, and the size of the original pellet apparently shrank after 11 h of electrolysis because of the removal of oxygen.

The element distributions of Fe and Ni were characterized by an EDX element mapping analysis (Fig. 9). The Fe and Ni

Fig. 8. Digital photos of mixed NiO and Fe_2O_3 pellets before (left) and after (right) electrolysis at 750°C with a cell voltage of 1.9 V in a Na_2CO_3–K_2CO_3 eutectic melt for 11 h.

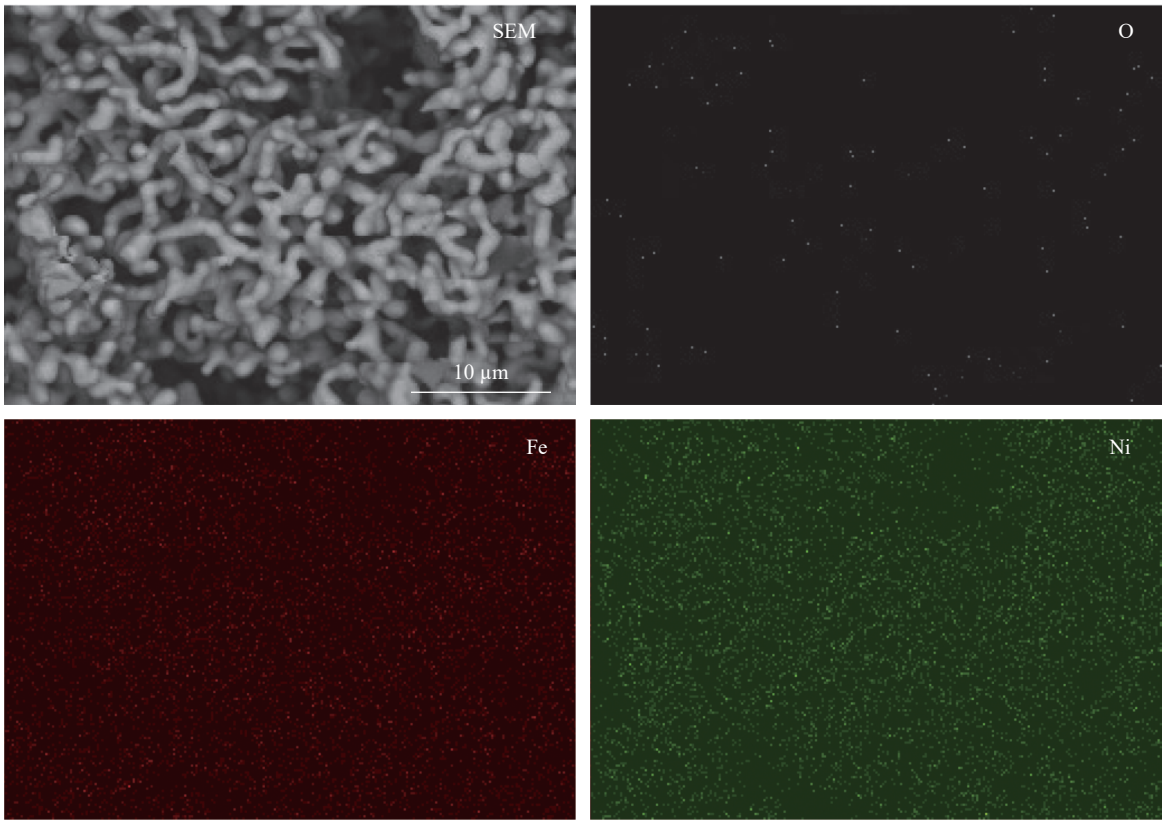

Fig. 9. Elemental distribution maps of the NiO and Fe_2O_3 mixed oxides pellet after electrolysis under a cell voltage of 1.9 V for 11 h at 750°C in a Na_2CO_3–K_2CO_3 eutectic melt.

were distributed uniformly, further confirming that they underwent a full alloying process. Therefore, the electrochemical alloying process was realized in the electro-deoxidation process at a relatively low temperature. Note that a small amount of element O was present because of the surface oxidation when the electrolytic pellet was exposed to the air and water.

Current–time plots recorded from the electrochemical reduction of the mixed oxides pellets under different cell voltages are shown in Fig. 10. All curves had several current plateaus before reaching a stable platform, suggesting that the reduction of the oxides pellets involved multiple steps, which agreed with the CV measurements. As with the XRD and CV analyses, the different plateaus should be due to the reduction of NiO, then electrochemical intercalation of Na^+ into iron oxide, and finally the reduction of $NaFe_2O_3$ and $NaFeO_2$ to generate Fe–Ni alloy. A higher cell voltage corresponded to a larger current and shorter reduction time.

The current efficiency and energy consumption of the electrolysis under different cell voltages are summarized in Table 1. Note that the energy used for heating the furnace was not included in the calculation of energy consumption of the electrolysis. The optimized current efficiency and energy consumption were achieved under a cell voltage of 1.9 V, and were 94.62% and 2.48 $kW{\cdot}h{\cdot}kg^{-1}$ for production of FeNi36

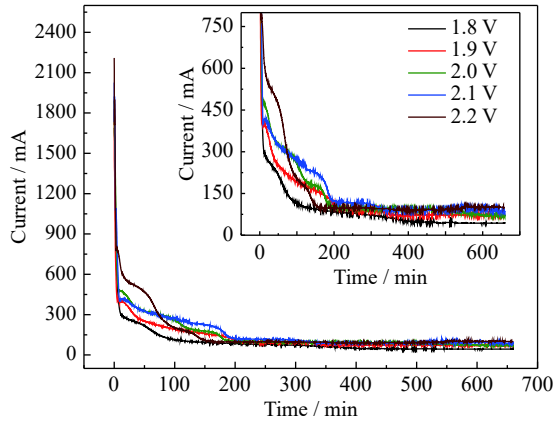

Fig. 10. Current–time plots of NiO and Fe_2O_3 mixed oxides pellets electrolyzed under different cell voltages for 11 h at 750°C in a Na_2CO_3–K_2CO_3 eutectic melt. Inset shows the partial drawing.

alloy, respectively. More importantly, the Ni10Cu11Fe alloy anode can produce oxygen during electrolysis [24]. The alloy anode survived over 800 h without any dimensional change upon consecutive electrolysis experiments in molten carbonates. This result further confirmed the inert nature of the alloy anode, enabling a low-emission electrolysis process in molten carbonates.

Table 1. Current efficiency and energy consumption for electro-reduction of NiO and Fe_2O_3 mixed oxides pellets under different electrolytic conditions

Electrolytic conditions	Mass of Fe_2O_3 and NiO / g	Actual consumed electric quantity / ($mA \cdot h^{-1}$)	Current efficiency / %	Energy consumption / ($kW \cdot h \cdot kg^{-1}$)
1.9 V, 11 h	1.4251	1286.5	94.62	2.48
2.0 V, 11 h	1.6365	1477.4	91.39	2.70
2.1 V, 11 h	1.6077	1451.4	88.35	2.94
2.2 V, 11 h	1.3806	1246.3	71.62	3.80

4. Conclusion

The Fe–Ni36 alloy was successfully prepared by electro-deoxidation of Fe_2O_3–NiO precursors using a one-step process in molten Na_2CO_3–K_2CO_3 at 750°C. After sintering, the oxide precursor consisted of $NiFe_2O_4$ and Fe_2O_3. During the electrolysis, Ni was preferentially extracted by electrochemical reduction of $NiFe_2O_4$, and then the reduction of iron oxides and formation of Ni–Fe alloy simultaneously occurred. No pure iron phase was observed during the electrolysis. The particle size of the obtained Fe–Ni36 alloy was smaller than those of iron and nickel, and Ni distributed uniformly in the Fe matrix. Under a constant cell voltage of 1.9 V, a current efficiency of 94.6% and an energy consumption of 2.48 $kW \cdot h \cdot kg^{-1}$ for production of FeNi36 alloy were achieved. The present study provides an energy-effective and low-emission approach to prepare Fe–Ni36 with the assistance of a low-cost inert anode at an intermediate temperature, and this method can also be used to prepare the other Fe-based alloys.

Acknowledgements

This work was financially supported by the National Natural Science Foundation of China (Nos. 51874211 and 51325102).

References

[1] W.D. Callister, *Materials Science and Engineering: An Introduction*, 7th ed., John Wiley & Sons, Inc., Hoboken, NJ, 2007, p. 1.

[2] T. Nagayama, T. Yamamoto, T. Nakamura, and Y. Fujiwara, Properties of electrodeposited invar Fe–Ni alloy/SiC composite film, *Surf. Coat. Technol.*, 322(2017), p. 70.

[3] T. Nagayama, T. Yamamoto, and T. Nakamura, Thermal expansions and mechanical properties of electrodeposited Fe–Ni alloys in the Invar composition range, *Electrochim. Acta*, 205(2016), p. 178.

[4] S.K. Sharma, F.J. Vastola, and P.L. Walker Jr., Reduction of nickel oxide by carbon: III. Kinetic studies of the interaction between nickel oxide and natural graphite, *Carbon*, 35(1997), No. 4, p. 535.

[5] G.Z. Chen, D.J. Fray, and T.W. Farthing, Direct electrochemical reduction of titanium dioxide to titanium in molten calcium chloride, *Nature*, 407(2000), No. 6802, p. 361.

[6] A.M. Abdelkader, K.T. Kilby, A. Cox, and D.J. Fray, DC voltammetry of electro-dexoidation of solid oxides, *Chem. Rev.*, 113(2013), No. 5, p. 2863.

[7] W. Xiao and D.H. Wang, The electrochemical reduction processes of solid compounds in high temperature molten salts, *Chem. Soc. Rev.*, 43(2014), No. 10, p. 3215.

[8] M. Ma, D.H. Wang, X.H. Hu, X.B. Jin, and G.Z. Chen, A direct electrochemical route from ilmenite to hydrogen-storage ferrotitanium alloys, *Chem. Eur. J.*, 12(2006), No. 19, p. 5075.

[9] S.Q. Jiao, L.L. Zhang, H.M. Zhu, and D.J. Fray, Production of NiTi shape memory alloys via electro-deoxidation utilizing an inert anode, *Electrochim. Acta*, 55(2010), No. 23, p. 7016.

[10] Y. Zhu, M. Ma, D.H. Wang, K. Jiang, X.H. Hu, X.B. Jin, and G.Z. Chen, Electrolytic reduction of mixed solid oxides in molten salts for energy efficient production of the TiNi alloy, *Chin. Sci. Bull.*, 51(2006), No. 20, p. 2535.

[11] G.H. Qiu, D.H. Wang, X.B. Jin, and G.Z. Chen, Preparation of Tb_2Fe_{17} by direct electrochemical reduction of Tb_4O_7–Fe_2O_3 pellet in molten calcium chloride, *Acta Metall. Sinica*, 44(2008), No. 7, p. 859.

[12] Y. Zhu, D.H. Wang, M. Ma, X.H. Hu, X.B. Jin, and G.Z. Chen, More affordable electrolytic $LaNi_5$-type hydrogen storage powders, *Chem. Commun.*, 2007, No. 24, p. 2515.

[13] G.H. Qiu, D.H. Wang, X.B. Jin, and G.Z. Chen, A direct electrochemical route from oxide precursors to the terbium–nickel intermetallic compound $TbNi_5$, *Electrochim. Acta*, 51(2006), No. 26, p. 5785.

[14] H.Y. Yin, T. Yu, D.Y. Tang, X.F. Ruan, H. Zhu, and D.H. Wang, Electrochemical preparation of NiAl intermetallic compound from solid oxides in molten $CaCl_2$ and its corrosion behaviors in NaCl aqueous solution, *Mater. Chem. Phys.*, 133(2012), No. 1, p. 465.

[15] A. Cox and D.J. Fray, Electrolytic formation of iron from haematite in molten sodium hydroxide, *Ironmaking Steelmaking*, 35(2008), No. 8, p. 561.

[16] H.Y. Yin, D.Y. Tang, H. Zhu, Y. Zhang, and D.H. Wang, Production of iron and oxygen in molten K_2CO_3–Na_2CO_3 by electrochemically splitting Fe_2O_3 using a cost affordable inert anode, *Electrochem. Commun.*, 13(2011), No. 12, p. 1521.

[17] X.H. Cheng, D.Y. Tang, D.D. Tang, H. Zhu, and D.H. Wang, Cobalt powder production by elecro-reduction of Co_3O_4 granules in molten carbonates using an inert anode, *J. Electrochem. Soc.*, 162(2015), No. 6, p. E68.

[18] D.Y. Tang, H.Y. Yin, X.H. Cheng, W. Xiao, and D.H. Wang, Green production of nickel powder by electro-reduction of NiO in molten Na_2CO_3–K_2CO_3, *Int. J. Hydrogen Energy*, 41(2016), No. 41, p. 18699.

[19] A. Cox and D.J. Fray, Mechanistic investigation into the electrolytic formation of iron from iron(III) oxide in molten sodium hydroxide, *J. Appl. Electrochem.*, 38(2008), No. 10, p. 1401.

[20] H.Y. Yin, X.H. Mao, D.Y. Tang, W. Xiao, L.R. Xing, H. Zhu, D.H. Wang, and D.R. Sadoway, Capture and electrochemical conversion of CO_2 to value-added carbon and oxygen by mol-

ten salt electrolysis, *Energy Environ. Sci.*, 6(2013), No. 5, p. 1538.

[21] X.H. Cheng, H.Y. Yin, and D.H. Wang, Rearrangement of oxide scale on Ni–11Fe–10Cu alloy under anodic polarization in molten Na_2CO_3–K_2CO_3, *Corros. Sci.*, 141(2018), p. 168.

[22] D.Y. Tang, K.Y. Zheng, H.Y. Yin, X.H. Mao, D.R. Sadoway, and D.H. Wang, Electrochemical growth of a corrosion-resistant multi-layer scale to enable an oxygen-evolution inert anode in molten carbonate, *Electrochim. Acta*, 279(2018), p. 250.

[23] D.Y. Tang, H.Y. Yin, W. Xiao, H. Zhu, X.H. Mao, and D.H. Wang, Reduction mechanism and carbon content investigation for electrolytic production of iron from solid Fe_2O_3 in molten K_2CO_3–Na_2CO_3 using an inert anode, *J. Electroanal. Chem.*, 689(2013), p. 109.

[24] K.Y. Zheng, K.F. Du, X.H. Chen, R. Jiang, B.W. Deng, H. Zhu, and D.H. Wang, Nickel–iron–copper alloy as inert anode for ternary molten carbonate electrolysis at 650°C, *J. Electrochem. Soc.*, 165(2018), No. 11, p. E572.